2012

Surface-enhanced Raman spectroscopy studies of organophosphorous model molecules and pesticides

PHYSICAL CHEMISTRY CHEMICAL PHYSICS, CAMBRIDGE, v. 14, n. 45, pp. 15645-15651, DEC, 2012

http://www.producao.usp.br/handle/BDPI/36488

PCCP

Cite this: *Phys. Chem. Chem. Phys.*, 2012, **14**, 15645–15651

www.rsc.org/pccp

PAPER

Surface-enhanced Raman spectroscopy studies of organophosphorous model molecules and pesticides

Jean C. S. Costa,[a] Romulo A. Ando,[a] Antônio C. Sant'Ana[b] and Paola Corio*[a]

Received 20th July 2012, Accepted 19th September 2012
DOI: 10.1039/c2cp42496g

This work reports the analytical application of surface-enhanced Raman spectroscopy (SERS) in the trace analysis of organophosphorous pesticides (trichlorfon and glyphosate) and model organophosphorous compounds (dimethyl methylphosphonate and *o*-ethyl methylphosphonothioate) bearing different functional groups. SERS measurements were carried out using Ag nanocubes with an edge square dimension of *ca.* 100 nm as substrates. Density functional theory (DFT) with the B3LYP functional was used for the optimization of ground state geometries and simulation of Raman spectra of the organophosphorous compounds and their silver complexes. Adsorption geometries and marker bands were identified for each of the investigated compound. Results indicate the usefulness of SERS methodology for the sensitive analyses of organophosphorous compounds through the use of vibrational spectroscopy.

Introduction

Surface-enhanced Raman scattering (SERS) is a powerful analytical tool strongly tied to plasmonics, a field that profits from the optical enhancement in nanostructures (usually metallic) that support localized surface plasmons. The focus has now turned towards realizing this potential in a host of applications.[1,2] Among the possible applications of SERS, the study of environmentally relevant species is of significant interest. This work reports the analytical application of SERS in the trace analysis of organophosphorous pesticides (trichlorfon and glyphosate) and model organophosphorous compounds bearing different functional groups on silver nanocubes aqueous suspensions.

Since the report of the single molecule SERS spectra in 1997 by Nie and Emory[3] and Kneipp *et al.*[4] there have been a boom of papers concerning the construction of nanostructured metallic substrates aiming to get the ultimate analytical tool. Such SERS-active surfaces, built with refined control over the size and shape of the nanostructures, present higher Raman enhancement factors than the traditional SERS substrates such as activated electrodes or aggregated colloids. The sensitivity and reproducibility of the Raman signal can significantly increase by the use of metallic nanoparticles with adequate size, shape and geometrical disposition over a substrate. These include nanoshells,[5,6] nanostars,[7] nanoholes,[8] nanocubes[9] and many others. Seminal reviews discuss the mechanisms involved in the SERS enhancement, and the correlation between such effect and the geometric properties of the metallic nanostructures, such as their aspect ratio and the presence of edges.[10–13]

When SERS experiments are performed under single molecule conditions, the estimated enhancement factor lies within the 10^7–10^{10} range.[14] Under such conditions there is a variation in the spectral pattern, since the observed signal is not an average result.[15] Above a certain limit of the adsorbate concentration on the surface, where an average SERS spectrum can be obtained, the use of a regular and ordered metallic substrate allows us to quantify the mother-solution concentration, making possible the analytical use of such a technique and the detection of species in trace levels. As a consequence, the use of the SERS technique has been gaining increasing importance to analytical applications in areas such as environmental,[16] biological[17] and forensic chemistry.[18]

Although organophosphorous compounds are widely used as pesticides and herbicides, SERS investigations of such a class of compounds are rare.[19] Such a class of compounds includes phosphines, phosphonates and phosphonothioates. In this work the SERS spectra of organophosphorous compounds bearing different functional groups (P═O and P═S) adsorbed on nanostructured silver SERS substrates were investigated. The studied adsorbates include dimethyl methylphosphonate (DMMP) and *o*-ethyl methylphosphonothioate (EMPT) as model molecules, as well as the widely used pesticides trichlorfon (dimethyl 2,2,2-trichloro-1-hydroxyethylphosphonate) and glyphosate (*N*-(phosphonomethyl)glycine). Trichlorfon is a common organophosphate insecticide that can act as a cholinesterase inhibitor altering the organism behavior, being frequently detected on surface runoff water from agricultural fields.[20] Glyphosate controls weeds by inhibiting the synthesis

[a] *Instituto de Química – Universidade de São Paulo, São Paulo, SP, Brazil. E-mail: jean-cla@iq.usp.br, raando@iq.usp.br, paola@iq.usp.br*
[b] *Departamento de Química – Universidade Federal de Juiz de Fora, Juiz de Fora, MG, Brazil. E-mail: antonio.sant@ufjf.edu.br*

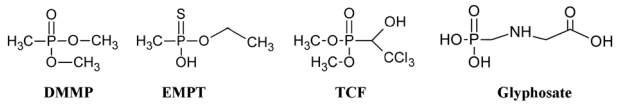

Fig. 1 Molecular structures of dimethyl methylphosphonate (DMMP), *o*-ethyl methylphosphonothioate (EMPT), trichlorfon (TCF) and glyphosate.

of aromatic amino acids necessary for protein formation in susceptible plants, and is among the most commonly world-wide used herbicides.[21,22] Fig. 1 shows the molecular structures of the investigated molecules.

The vibrational assignment for the Raman and SERS spectra of the organophosphorous compounds was achieved by comparing the Density Functional Theory (DFT) simulated Raman spectra of the molecules when isolated or attached to a silver atom. The relative intensities of the bands from SERS spectra differed significantly from those of Raman spectra owing to the specific surface selection rules[23] associated with the eventual surface-complex formation. Comparison between the Raman spectra of the compounds in the solid-state with the SERS spectra of such molecules adsorbed on silver nanoparticle surfaces allowed the characterization of the interaction between the adsorbates and the metallic surface. In fact, the understanding of the interaction between target analytes and the surface of metallic nanostructures is essential for the interpretation of SERS spectra.[24] The assignment of the strongest SERS bands from the model molecules DMMP and EMPT, which are generally related to the adsorption sites, allowed the understanding of the adsorption geometry of trichlorfon and glyphosate. The identification of these bands is important prior to the use of the SERS technique as an analytical tool for such environmentally relevant species.

Experimental

Materials and instrumentation

UV–VIS spectra were obtained from aqueous suspensions containing the Ag nanocubes using a Shimadzu UVPC-3101 spectrophotometer. Raman spectra were acquired on a Renishaw Raman InVia equipped with a CCD detector and coupled to a Leica microscope that allows a rapid accumulation of Raman spectra with a spatial resolution of about 1 μm (micro-Raman technique). The laser beam was focused on the sample using a 50× lens. The laser power was always kept below 0.7 mW at the sample. The experiments were performed under ambient conditions using a back-scattering geometry. The samples were irradiated with the 632.8 nm line of a He–Ne laser (Renishaw RL633 laser). The scanning electron microscopy (FEG-SEM) images were obtained with a JEOL microscope (Mod.: FEG-SEM JSM 6330F) operated at 5 kV. The samples for SEM were prepared by drop-casting an aqueous suspension of the nanostructures over a Si wafer, followed by drying under ambient conditions.

Analytical grade chemicals and solvents were supplied by Aldrich and Merck, and were used as received. All solutions were prepared using deionized water (18.2 MΩ). Glassware was cleaned with a 3 : 1 concentrated H_2SO_4 to 30% H_2O_2 aqueous solution before use.

Silver nanocube synthesis

Silver nanocubes were prepared by modification of the reported synthesis proposed by Xia *et al.*[25,26] Briefly, 3 mL of a solution of $AgNO_3$ in ethylene glycol (0.25 mol L^{-1}) and an equal volume of 0.375 mol L^{-1} polyvinylpyrrolidone (PVP) solution in ethylene glycol was added, using a peristaltic pump at a rate of 0.4 mL min^{-1}, to 5 mL of anhydrous ethylene glycol at 160 °C, under stirring. The temperature was kept constant for 1 h. The resulting suspension was centrifuged and the recovered solid redispersed in water.

Sample preparation for SERS

The samples were prepared by adding 100 μL of the suspension containing the Ag nanocubes to 50 μL of 1.0×10^{-6} mol L^{-1} organophosphorous aqueous solutions. The resulting silver and organophosphorous concentration were 4.5×10^{-2} mol L^{-1} and 3.3×10^{-7} mol L^{-1}, respectively. The SERS spectra were obtained 1 h after the sample preparation, in order to ensure that the adsorption equilibrium of the analytes over the metallic surfaces was reached.

Computational details

The quantum chemical calculations were performed with the aid of the Gaussian 03 software[27] for the organophosphorous compounds and for the molecules attached to an Ag atom. The ground state geometries were fully optimized employing the density functional theory (DFT)[28–30] with the B3LYP hybrid functional (Becke's gradient-corrected exchange correlation in conjunction with the Lee–Yang–Parr correlation functional with three parameters) and the 6-311++G(d,p) one-electron atomic basis sets. The calculations of the molecules attached to Ag atoms were performed using the gen keyword where the light atoms (CHNOPS) were calculated with the 6-311++G(d,p) basis set and the Ag atoms with the LANL2DZ basis set considering a pseudo potential. The vibrational frequency analyses were carried out and no imaginary frequencies were found, indicating that the optimized geometries were in a minimum of the potential energy surface.

Results and discussion

Substrate characterization

Fig. 2(a) presents a SEM image of the silver nanocubes synthesized *via* the polyol approach, where a mean edge square dimension of *ca.* 100 nm is observed. The extinction spectrum of an ensemble of silver nanocubes in water is shown in

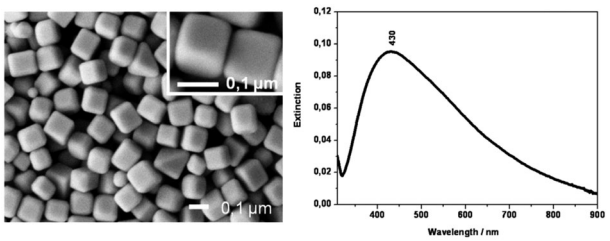

Fig. 2 (a) SEM images obtained from silver nanocubes supported on the Si wafer. (b) Extinction spectrum of silver nanocubes aqueous suspension.

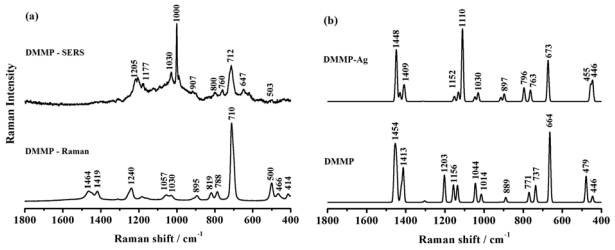

Fig. 3 (a) Raman spectrum of solid state DMMP (bottom trace) and the SERS spectrum of 3.3×10^{-7} mol L^{-1} DMMP on Ag nanocubes (upper trace) obtained at $\lambda_{exc.} = 632.8$ nm; (b) calculated spectra of solid-sate DMMP and DMMP–Ag considering the adsorption of DMMP on an Ag atom through the methoxy group.

Fig. 2(b). The localized surface plasmon resonance (LSPR) band is broad and intense, with maximum at *ca.* 430 nm, suggesting a suitable size distribution for SERS experiments in the visible spectral region. This dipole LSPR band position is consistent with previous studies of nanocube structures.[31] The Ag nanocubes were employed as substrates for the SERS study of organophosphorous model compounds and pesticides.

SERS of model compounds: DMMP and EMPT over silver nanocubes

Fig. 3(a) shows the comparison of the SERS spectrum of DMMP obtained by using Ag nanocubes with its corresponding Raman spectrum. Fig. 3(b) shows the calculated Raman spectra for the DMMP and the DMMP–Ag complex. The vibrational assignment for the main Raman bands based on DFT calculations is presented in Table 1.

The most intense bands present in the DMMP Raman spectrum are also present in its SERS spectrum. However, changes in both relative intensities and the position of the bands are observed, suggesting chemical adsorption of the molecule to the nanoparticle surface. The intense bands in the Raman spectrum located at 500 cm^{-1} (assigned to $\delta(PO_3)$ umbrella), 710 cm^{-1} (assigned to $\nu(P–CH_3)$ stretching + $\nu(P–O)$ stretching + $\delta(P–O–CH_3)$ bending), 1419 cm^{-1} (assigned to $\delta(CH_3)$ bending) and 1464 cm^{-1} (assigned to $\delta(CH_3)$ bending) show a significant decrease in intensity in the SERS spectrum. The adsorption of the DMMP onto the nanostructured surface causes the appearance in the SERS spectrum of a sharp and intense band at 1000 cm^{-1}, which is assigned to $\nu(P{=}O)$ stretching + $\delta(CH_3)$ and a shift from 1240 cm^{-1} to 1205 cm^{-1} of the band assigned to $\nu(P{=}O)$ stretching + $\delta(CH_3)$. Such changes in the spectral pattern are corroborated by the theoretical spectra obtained by the DFT calculations. The intense SERS band at 1000 cm^{-1} appears at 1110 cm^{-1} in the calculated Raman spectrum of the Ag complex. The discrepancies observed in the experimental and theoretical wavenumbers show that the DFT calculations do not properly describe the P–O and P=O bond orders. It can be observed that the modes involving the $\nu(P–O)$ are underestimated in comparison to the experimental values, while the $\nu(P{=}O)$ is overestimated (Table 1). Such spectral changes suggest an adsorption geometry where the molecule interacts with the surface primarily by the oxygen atom from the P=O bond as shown in Fig. 4.

Table 1 Tentative assignment of the experimental Raman and SERS bands and calculated wavenumbers for DMMP and Ag–DMMP species

Raman	Calculated DMMP	SERS Ag	Calculated DMMP–Ag	Tentative assignment
466	446	437	446	$\delta(P–O–CH_3)$
500	479	503	455	$\delta(PO_3)_{umbrella}$
710	664	712	673	$\nu(P–CH_3) + \nu(P–O) + \delta(P–O–CH_3)$
788	737	760	763	$\nu_{as}(O–P–O)$
819	771	800	796	$\nu(P–CH_3)$
895	889	907	897	$\delta(CH_3)$
—	—	1000	1110	$\nu(P{=}O) + \delta(CH_3)$
1028	1014	1030	1030	$\nu(O–CH_3) + \nu_{as}(O–P–O)$
1057	1044	—	1047	$\nu(O–CH_3) + \nu_s(O–P–O)$
1179	1156	1177	1152	$\delta(CH_3)$
1240	1203	1205	—	$\nu(P{=}O) + \delta(CH_3)$
1419	1413	—	1409	$\delta(CH_3)$
1464	1454	—	1448	$\delta(CH_3)$

τ = twisting; ν = stretching; ω = wagging; δ = bending; ρ = rocking.

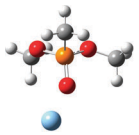

Fig. 4 Optimized geometry for the DMMP adsorbed on an Ag atom.

Fig. 5(a) shows the comparison of SERS spectra of EMPT obtained by using Ag nanocubes with the corresponding Raman spectrum of the compound in the solid state. The main differences observed are the splitting of the band at 593 cm^{-1} in the Raman spectrum to 553 cm^{-1} and 601 cm^{-1} in the SERS spectrum, both assigned to the stretching of P=S + bending of O–P–O bonds. Fig. 5(b) shows the calculated Raman spectra for the EMPT and EMPT–Ag considering two possible adsorption species, the protonated (EMPT–Ag) and the deprotonated ($EMPT^+$–Ag) (Fig. 6). In fact, the calculated Raman spectrum of the complexes shows a shift of the band assigned to the $\nu(P{=}S) + \delta(O–P–O)$ mode from 575 cm^{-1} to 512 cm^{-1} and 527 cm^{-1}, for $EMPT^+$–Ag and EMPT–Ag, respectively. Such a spectral pattern suggests that the increase in the P=O bond order is caused by the decrease

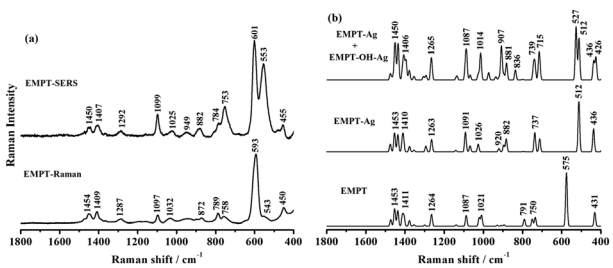

Fig. 5 (a) Raman spectrum of solid state EMPT (bottom trace) and the SERS spectrum of 3.3×10^{-7} mol L^{-1} EMPT on Ag nanocubes (upper trace) obtained at $\lambda_{exc.} = 632.8$ nm; (b) calculated spectra of isolated EMPT and coordinated with an Ag atom as deprotonated and neutral species.

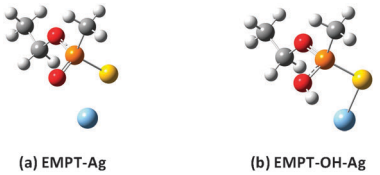

Fig. 6 Optimized geometries for the EMPT adsorbed on an Ag atom according to the following possibilities: (a) in deprotonated and (b) neutral forms.

Table 2 Tentative assignment of the experimental Raman and SERS bands and calculated wavenumbers for EMPT species

Raman	Calculated EMPT	SERS Ag	Calculated EMPT–Ag	Tentative assignment
450	431	455	437	δ(C–P–O)
593	575	553	512	ν(P═S) + δ(O–P–O)
—	—	601	—	ν(P═S) + δ(O–P–O)
758	750	753	712	ν(P–CH_3)
789	791	784	737	ν(P–O) + $\delta(CH_3)$
872	894	882	882	$\delta(CH_3)$
1032	1021	1025	1028	δ(OH) + ν(O–C)
1097	1087	1099	1091	ν(C–C) + $\tau(CH_3)$
1287	1264	1292	1263	$\delta(CH_3)$
1409	1411	1407	1410	$\delta(CH_3)$ + $\tau(CH_3)$
1454	1453	1450	1453	$\tau(CH_3)$

τ = twisting; ν = stretching; ω = wagging; δ = bending; ρ = rocking.

in the P═S bond order when the coordination with the silver occurs. On the other hand, this result cannot explain the splitting observed in the SERS spectrum, which allows suggesting the adsorption of both species takes place. Fig. 5(b) shows the sum of the calculated spectra for both $EMPT^+$–Ag and EMPT–Ag species. The band at 527 cm^{-1}, observed in the theoretical spectrum of the latter which is presented at 601 cm^{-1} in the SERS spectrum indicates the low double bond character of the P–O bond in the protonated species. The difference in the wavenumber, as in DMMP discussion, can be explained by the difficulty of the DFT method to calculate the ligand–metal charge transfer. In the SERS spectrum, the relative small enhancement of the bands at 753, 784 and 1099 cm^{-1} and small shifts of all bands greater than 700 cm^{-1} are observed in the theoretical spectra, reinforcing our hypothesis. The observed bands, as well as the vibrational assignment performed based on DFT calculations are summarized in Table 2.

SERS of pesticides: trichlorfon and glyphosate over silver nanocubes

Fig. 7 shows the Raman spectrum of the herbicide trichlorfon (TCF) in the solid state and its SERS spectrum when adsorbed on the silver nanocubes surface, and the respective calculated Raman spectra. The main vibrational modes for trichlorfon based on DFT calculations are presented in Table 3. In a previous paper we showed the SERS spectrum of TCF over Au nanorods,[32] and the main conclusion was that the TCF interacts with the Au surface by the oxygen atoms from the hydroxy and methoxy groups and not by the oxygen from the

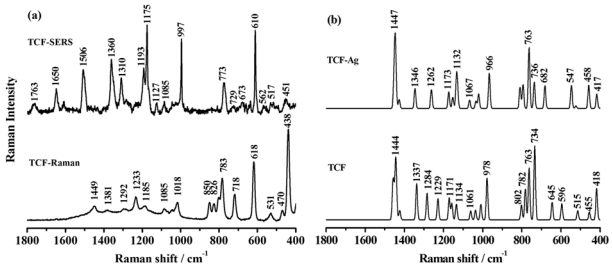

Fig. 7 (a) Raman spectrum of solid state TCF (bottom trace) and the SERS spectrum of 3.3×10^{-7} mol L^{-1} TCF on Ag nanocubes (upper trace) obtained at $\lambda_{exc.}$ = 632.8 nm; (b) calculated spectra of solid-sate TCF and TCF–Ag.

Table 3 Tentative assignment of the experimental Raman and SERS bands and calculated wavenumbers for trichlorfon

Raman	Calculated TCF	SERS Ag	Calculated TCF-Ag	Tentative assignment
438	418	438	417	ν(C–Cl) + δ(P═O–C)
470	455	451	458	δ(O–P═O)
531	515	517	524	$\delta(P{=}O_3)$
—	—	562	547	ν(CCl) + δ(C–P)
618	645	610	682	ν(C–Cl) + ν(P–C) + δ(O–H)
718	734	729	736	ν(P═O) + ν(C–Cl)
783	763	773	763	ν(C–Cl) + δ(C–C–P)
826	782	—	794	ν(C–Cl) + δ(OH) + ν(C–P)
850	802	—	809	ν(P–O) + ν(O–CH_3) + ν(C–OH)
1018	978	997	966	ν(C–C) + δ(OH)
1085	1061	1085	1067	ν(C–OH)
	—	1175	1132	$\tau(CH_3)$ + ν(P═O)
1181	1158	—	—	$\tau(CH_3)$
1185	1171	1193	1173	δ(OH) + δ(CH)
1233	1229	—	—	δ(OH) + δ(CH) + ν(P═O)
1292	1284	1310	1262	δ(CH) + δ(OH)
1381	1337	1360	1346	δ(CH) + δ(OH)
1449	1444	—	1447	$\delta(CH_3)$
—	—	1506	—	—
—	—	1650	—	—
—	—	1763	—	—

τ = twisting; ν = stretching; ω = wagging; δ = bending; ρ = rocking.

P═O bond. However, in the case of the interaction of TCF with Ag nanocubes, it is observed a very different spectral pattern in comparison to the one observed by adsorption over the Au surface. The main difference is the appearance of an intense band at 1175 cm^{-1} in the SERS spectrum of TCF adsorbed over the Ag surface that according to the DFT calculations can be assigned to the $\delta(CH_3)$ + ν(P═O) mode. Thus, in the case of the Ag surface, it is suggested that the interaction involves the oxygen atom of the P═O bond as illustrated in Fig. 8. The

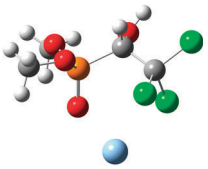

Fig. 8 Optimized geometry for the TCF adsorbed on an Ag atom.

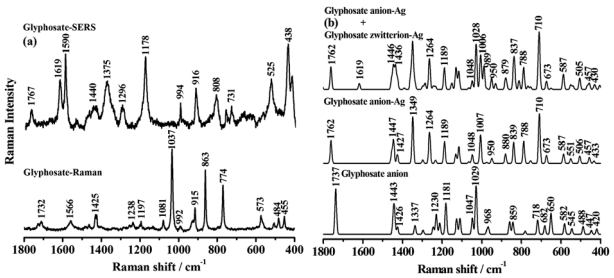

Fig. 9 (a) Raman spectrum of glyphosate in the solid state (bottom trace) and the SERS spectrum of 3.3×10^{-7} mol L^{-1} glyphosate on Ag nanocubes (upper trace) obtained at $\lambda_{exc.} = 632.8$ nm; (b) calculated spectra of solid-sate glyphosate and glyphosate–Ag.

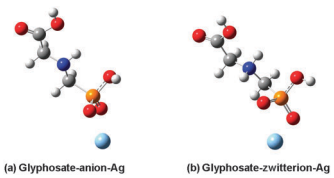

Fig. 10 Optimized geometries for the glyphosate adsorbed on an Ag atom according to the following possibilities: (a) in anionic and (b) zwitterionic forms.

intense SERS bands at 610 and 773 cm^{-1}, assigned to vibrational modes involving the stretching of C–Cl bonds, as well as the enhanced bands at 997 cm^{-1}, assigned to the stretching of the C–C bond, suggest the proximity of such groups to the silver surface, in agreement with the calculated spectrum obtained from the proposed coordination geometry.

Fig. 9 shows the Raman spectrum of glyphosate in the solid state and the SERS spectrum of such compound adsorbed on silver nanocube surfaces, as well as the respective calculated spectra. It is observed that the SERS spectrum of glyphosate differs significantly from its characteristic Raman spectrum in the solid state. As the acid–base equilibrium of glyphosate species in solution involves several species,[33] it is quite reasonable that more than one species should adsorb on the Ag surface. In fact, the theoretical calculations suggest that there is adsorption of the anionic and zwitterionic species (Fig. 10).

The main vibrational bands with the corresponding tentative assignment for the glyphosate anion based on DFT calculations are shown in Table 4. The vibrational assignment of the zwitterionic species (not shown in the table) is similar to the other species, where the main difference is the bending mode of NH_2^+, $\delta(NH_2^+)$, which appears at *ca.* 1619 cm^{-1}.

Comparing the Raman and the SERS spectra, it is observed a decrease in the most intense bands, particularly the band at 1037 cm^{-1}, assigned to a mode involving the symmetric stretching of PO_2, $\nu_s(PO_2)$, and an increase in the bands at 1178 and 1375 cm^{-1}, assigned to modes involving the CH_2 moieties. This is in accordance with the adsorption of the anionic species (Fig. 10a), where the calculated spectrum shows the disappearance of the band at 1029 cm^{-1} and the appearance of the characteristic bands at 1189 and 1349 cm^{-1}. Another evidence of the adsorption of the anionic species is the shift of the ν(C═O) mode to 1767 cm^{-1}, in accordance with the calculated value at 1762 cm^{-1}. On the other hand, it is observed in the SERS spectrum the appearance of two intense bands at 1619 and 1590 cm^{-1}, that are not present in the calculated Raman spectra of the anionic species. The band at 1619 cm^{-1}, assigned to $\delta(NH_2^+)$, is an indication that there is the co-adsorption of the zwitterionic species.

Several possibilities of adsorption were considered to calculate adsorption geometry of the glyphosate anionic and zwitterionic species, where the configurations that resulted in theoretical spectra with the best agreement with experimental data are illustrated in Fig. 10, which involves interaction *via* the phosphate group.

SERS marker bands of organophosphorous compounds

Considering the above described results, it is possible to identify sets of marker bands of the adsorption on silver for

Table 4 Tentative assignment of the experimental Raman and SERS bands and calculated wavenumbers for glyphosate

Raman (cm^{-1})	Calculated anionic form (cm^{-1})	SERS on Ag nanocubes (cm^{-1})	Calculated anionic form-Ag (cm^{-1})	Tentative assignment
455	438	438	457	$\rho(CH_2)$ + δ(OH)
484	488	—	506	δ(OH) + $\rho(CH_2)$ + (PO_2)
506	545	525	551	δ(OH) + δ(CH)
573	582	525	587	δ(OH) + δ(OH-C═O)
—	718	731	710	δ(NH) + ν(C–P)
774	781	762	788	δ(NH) + $\rho(CH_2)$ + ν(P–OH)
863	859	808	839	$\rho(CH_2)$ + δ(NH) + ν(C–C)
—	—	916	880	$\rho(CH_2)$
992	968	—	—	$\rho(CH_2)$ + δ(OH)
1037	1029	994	1007	$\nu_s(PO_2)$ + δ(OH)
1081	1047	–	1048	ν(C–N) + ν(C–OH)
1197	1181	1178	1189	$\tau(CH_2)$ + δ(OH)
1238	1230	—	1234	$\tau(CH_2)$
—	1245	1296	1264	$\omega(CH_2)$
—	1337	1375	1349	$\omega(CH_2)$ + ν(C–C)
1425	1426	—	1427	$\delta(CH_2)$
1433	1443	1440	1447	$\delta(CH_2)$
1566	—	1590	—	—
—	—	1619	1619[a]	$\delta(NH_2^+)$[a]
1732	1737	1767	1762	ν(C═O)

[a] The band at 1619 cm^{-1} is assigned to $\delta(NH_2^+)$ of the zwitterionic species. τ = twisting; ν = stretching; ω = wagging; δ = bending; ρ = rocking.

Table 5 Main set of marker bands identified in the SERS spectra for the investigated organophosphorous compounds

Compound	Characteristic SERS bands (cm^{-1})	Tentative assignment
DMMP (P═O)	712	ν(P–CH_3) + ν(P–O) + δ(P–O–CH_3)
	1000	ν(P═O) + δ(CH_3)
EMPT (P═S)	601	ν(P═S) + δ(O–P–O)
	753	ν(P–CH_3)
	1099	ν(C–C) + τ(CH_3)
Trichlorfon (P═O)	610	ν(C–C1) + ν(P–C) + δ(O–H)
	773	ν(C–C1) + δ(C–C–P)
	997	ν(C–C) + δ(OH)
Glyphosate	916	ρ(CH_2)
	1178	τ(CH_2) + δ(OH)
	1375	ω(CH_2) + ν(C–C)

the different investigated organophosphorous compounds, as shown in Table 5.

These bands are assigned to the adsorption sites in each species. It can be observed that the most intense SERS bands for each compound are in different wavenumbers, in spite of these compounds have closely related chemical structures. The presented results therefore suggest the usefulness of SERS methodology for the analyses of a multi-component mixture of organophosphorus compounds through the use of vibrational spectroscopy.

Conclusions

Silver nanocubes were successfully employed as substrates for the SERS study of organophosphorous model compounds and pesticides showing high sensitivity and selectivity. The use of SERS as an analytical tool requires the interpretation of SERS spectra of chemisorbed species, which are dependent on the vibrational assignment of the surface complex and of the surface selectivity. In this work, density functional theory (DFT) with the B3LYP functional allowed the reliable vibrational assignment for the Raman spectra of organophosphorous molecules in the solid state and the SERS spectra of such compounds adsorbed on the silver surface. Adsorption geometries and binding sites for the organophosporous compounds over the silver surface were identified using theoretical spectra considering several possibilities of adsorption, allowing the identification of the configuration that resulted in the best agreement with the experimental SERS result. The DMMP compound interacts with the surface primarily by the oxygen atom from the P═O bond, while EMPT adsorbs as both neutral and deprotonated species, involving mainly the P═S moiety. The SERS spectrum of trichlorfon suggests that chemisorption involves the oxygen atom of the P═O bond and chlorine groups, while for glyphosate, the phosphate group is identified as the main binding site, where there is adsorption of anionic and zwitterionic species.

Therefore, the assignment of the more intense bands from organophosphorous molecules adsorbed on silver surfaces, which in the SERS spectra can be related to the molecular site involved in the surface interaction, allows the identification of the adsorption mechanism. Such results are very important for the potential use of the SERS technique as an analytical tool for the identification of such a kind of molecules to satisfy environmental demands.

Acknowledgements

The authors gratefully acknowledge support from FAPESP, CNPq and CAPES.

Notes and references

1 N. P. W. Pieczonka and R. F. Aroca, *Chem. Soc. Rev.*, 2008, **37**, 946.
2 R. Aroca, *Surface-enhanced Vibrational Spectroscopy*, John Wiley & Sons, Chichester, 2006.
3 S. Nie and S. R. Emory, *Science*, 1997, **275**, 1102.
4 K. Kneipp, Y. Wang, H. Kneipp, L. T. Perelman, I. Itzkan, R. R. Dasari and M. S. Feld, *Phys. Rev. Lett.*, 1997, **78**, 1667.
5 S. Lal, N. K. Grady, J. Kundu, C. S. Levin, J. B. Lassiter and N. J. Halas, *Chem. Soc. Rev.*, 2008, **37**, 898.
6 C. M. S. Izumi, M. G. Moffitt and A. G. Brolo, *J. Phys. Chem. C*, 2011, **115**, 19104.
7 L. Rodriguez-Lorenzo, R. A. Alvarez-Puebla, F. J. G. Abajo and L. M. Liz-Marzan, *J. Phys. Chem. C*, 2010, **114**, 7336.
8 R. Gordon, D. Sinton, K. L. Kavanagh and A. G. Brolo, *Acc. Chem. Res.*, 2008, **41**, 1049.
9 J. M. McLellan, Z. Li, A. R. Siekkinen and Y. Xia, *Nano Lett.*, 2007, **7**, 1013.
10 P. L. Stiles, J. A. Dieringer, N. C. Shah and R. P. Van Duyne, *Annu. Rev. Anal. Chem.*, 2008, **1**, 601.
11 X. Lu, M. Rycenga, S. E. Skrabalak, B. Wiley and Y. Xia, *Annu. Rev. Phys. Chem.*, 2009, **60**, 167.
12 M. J. Banholzer, J. E. Millstone, L. Qin and C. A. Mirkin, *Chem. Soc. Rev.*, 2008, **37**, 885.
13 M. J. Natan, *Faraday Discuss.*, 2006, **132**, 321; C. R. Yonzon, D. A. Stuart, X. Zhang, A. D. McFarland, C. L. Haynes and R. P. Van Duyne, *Talanta*, 2005, **67**, 438; K. Kneipp and H. Kneipp, *Acc. Chem. Res.*, 2006, **39**, 443; M. Moskovits, *J. Raman Spectrosc.*, 2005, **36**, 485.
14 E. C. Le Ru, E. Blackie, M. Meyer and P. G. Etchegoin, *J. Phys. Chem. C*, 2007, **111**, 13794.
15 N. P. W. Pieczonka and R. F. Aroca, *ChemPhysChem*, 2005, **6**, 2473.
16 R. A. Halvorson and P. Vikesland, *J. Environ. Sci. Technol.*, 2010, **44**, 7749; P. Leyton, S. Sanchez-Cortes, J. V. Garcia-Ramos, C. Domingo, M. Campos-Vallette, C. Saitz and R. E. Clavijo, *J. Phys. Chem. B*, 2004, **108**, 17484; L. He, M. J. Natan and C. D. Keating, *Anal. Chem.*, 2000, **72**, 5348; M. A. de Jesus, K. S. Giesfeld and M. J. Sepaniak, *J. Raman Spectrosc.*, 2004, **35**, 895.
17 X. Zhang, M. A. Young, O. Lyandres and R. P. Van Duyne, *J. Am. Chem. Soc.*, 2005, **127**, 4484; L. R. Hirsch, A. M. Gobin, A. R. Lowery, F. Tam, R. A. Drezek, N. J. Halas and J. L. West, *Ann. Biomed. Eng.*, 2006, **34**, 15.
18 B. Sagmuller, B. Schwarze, G. Brehm and S. Schneider, *Analyst*, 2001, **126**, 2066; J. M. Sylvia, J. A. Janni, J. D. Klein and K. M. Spencer, *Anal. Chem.*, 2000, **72**, 5834.
19 A. M. Alak and T. Vo-Dinh, *Anal. Chem.*, 1987, **59**, 2149.
20 G. Howe, L. L. Marking, T. D. Bills, J. J. Rach and F. L. Mayer Jr., *Environ. Toxicol. Chem.*, 1994, **13**, 51.
21 J. E. Franz, M. K. Mao and J. A. Sikorski, *Glyphosate, A Unique Global Herbicide*, American Chemical Society, Washington DC, 1997, p. 653.
22 E. M. D. Kirmser, D. O. Mártire, M. C. Gonzalez and J. A. Rosso, *J. Agric. Food Chem.*, 2010, **58**, 12858.
23 M. Moskovits, *Rev. Mod. Phys.*, 1985, **57**, 783.
24 J. C. S. Costa, R. A. Ando, P. H. C. Camargo and P. Corio, *J. Phys. Chem. C*, 2011, **115**, 4184.
25 Y. Sun and Y. Xia, *Analyst*, 2003, **128**, 686.
26 S. H. Im, Y. T. Lee, B. Wiley and Y. Xia, *Angew. Chem., Int. Ed.*, 2005, **44**, 2154.
27 M. J. Frisch, G. W. Trucks, H. B. Schlegel, G. E. Scuseria, M. A. Robb, J. R. Cheeseman, J. A. Montgomery, T. Vreven, K. N. Kudin, J. C. Burant, J. M. Millam, S. S. Iyengar, J. Tomasi,

V. Barone, B. Mennucci, M. Cossi, G. Scalmani, N. Rega, G. A. Petersson, H. Nakatsuji, M. Hada, M. Ehara, K. Toyota, R. Fukuda, J. Hasegawa, M. Ishida, T. Nakajima, Y. Honda, O. Kitao, H. Nakai, M. Klene, X. Li, J. E. Knox, H. P. Hratchian, J. B. Cross, V. Bakken, C. Adamo, J. Jaramillo, R. Gomperts, R. E. Stratmann, O. Yazyev, A. J. Austin, R. Cammi, C. Pomelli, J. W. Ochterski, P. Y. Ayala, K. Morokuma, G. A. Voth, P. Salvador, J. J. Dannenberg, V. G. Zakrzewski, S. Dapprich, A. D. Daniels, M. C. Strain, O. Farkas, D. K. Malick, A. D. Rabuck, K. Raghavachari, J. B. Foresman, J. V. Ortiz, Q. Cui, A. G. Baboul, S. Clifford, J. Cioslowski, B. B. Stefanov, G. Liu, A. Liashenko, P. Piskorz, I. Komaromi, R. L. Martin, D. J. Fox, T. Keith, M. A. Al-Laham, C. Y. Peng, A. Nanayakkara, M. Challacombe, P. M. W. Gill, B. Johnson, W. Chen, M. W. Wong, C. Gonzalez and J. A. Pople, *Gaussian 03, Revision D.01*, Gaussian, Inc., Wallingford CT, 2004.

28 D. J. Becke, *Chem. Phys.*, 1993, **985**, 648.

29 C. T. Lee, W. T. Yang and R. G. Parr, *Phys. Rev. B: Condens. Matter Mater. Phys.*, 1998, **37**, 785.

30 P. J. Stephens, F. J. Devlin, C. F. Chabalowski and M. J. Frisch, *J. Phys. Chem.*, 1994, **98**, 11623.

31 L. J. Sherry, S. Chang, G. C. Schatz, R. P. Van Duyne, B. J. Wiley and Y. Xia, *Nano Lett.*, 2005, **5**, 2034.

32 J. C. S. Costa, R. A. Ando, A. C. Sant'Ana, L. M. Rossi, P. S. Santos, M. L. A. Temperini and P. Corio, *Phys. Chem. Chem. Phys.*, 2009, **11**, 7491.

33 O. P. A. Junior, T. C. R. dos Santos, N. M. Brito and M. L. Ribeiro, *Quim. Nova*, 2002, **25**, 589.